

Competition of crystal field splitting and Hund's rule coupling in two-orbital magnetic metal-insulator transitions

Ya-Min Quan¹, Liang-Jian Zou^{1,2*}, Dayong Liu¹, and Hai-Qing Lin²

¹ Key Laboratory of Materials Physics,
Institute of Solid State Physics, Chinese Academy of Sciences,
P. O. Box 1129, Hefei 230031, China

² Department of Physics, Chinese University of Hong Kong,
Shatin, New Territory, Hong Kong, China

(Dated: Nov 4, 2011)

Competition of crystal field splitting and Hund's rule coupling in magnetic metal-insulator transitions of half-filled two-orbital Hubbard model is investigated by multi-orbital slave-boson mean field theory. We show that with the increase of Coulomb correlation, the system firstly transits from a paramagnetic (PM) metal to a *Néel* antiferromagnetic (AFM) Mott insulator, or a nonmagnetic orbital insulator, depending on the competition of crystal field splitting and the Hund's rule coupling. The different AFM Mott insulator, PM metal and orbital insulating phase are none, partially and fully orbital polarized, respectively. For a small J_H and a finite crystal field, the orbital insulator is robust. Although the system is nonmagnetic, the phase boundary of the orbital insulator transition obviously shifts to the small U regime after the magnetic correlations is taken into account. These results demonstrate that large crystal field splitting favors the formation of the orbital insulating phase, while large Hund's rule coupling tends to destroy it, driving the low-spin to high-spin transition.

PACS numbers: 71.30.+h, 75.30.Kz, 71.10.Hf, 71.27.+a, 71.10.Fd

I. INTRODUCTION

Mott-Hubbard metal-insulator transitions (MIT) in multi-orbital Hubbard models have been extensively studied since there are rich phase diagrams¹⁻¹². A few of many-body approaches have been employed to study the paramagnetic Mott transition, such as dynamic mean field theory (DMFT)¹⁻⁸ and Kotliar-Ruckenstein slave-boson method^{9,10}, *etc.* With the slave spin technique, Yu and Si recently showed that a paramagnetic orbital insulating phase can exist when the Hund's coupling approaches zero¹¹. However, generally speaking, MIT transitions are usually accompanied by magnetic transitions. How spin correlation affects the nature of MIT is seldom discussed.

On the other hand, the crystal field splitting plays an important role in the properties of multi-orbital systems. It is not clear whether the interplay between crystal field splitting and spin exchange splitting is a key factor for antiferromagnetic (AFM) MIT. Though Hasegawa¹³ studied the spin correlation effect in half-filled doubly degenerate Hubbard model and found the Hund's coupling plays a very considerable role in magnetization, he did not find the MIT at half filling. It deserves to explore the influence of crystal field splitting on the MIT in the presence of magnetism. And how the crystal field and spin correlation modify the orbital insulating phase is also an interesting issue.

In this paper, the multi-orbital Kotliar-Ruckenstein slave-boson method is generalized with spin degree of freedom. The effects of crystal field splitting and Hund's rule coupling on Mott transition are also discussed. We find that besides

$J_H = 0$, orbital insulator can exist for small enough but finite J_H , different from Yu and Si's results¹¹. The magnetic phase diagram as a function of U and crystal field splitting shows that the phase boundary can be seriously changed by the Hund's rule coupling and crystal field splitting, demonstrating the contrary role of these two factors. The rest of this paper is organized as follows: in Sec. II we describe the model Hamiltonian and theoretical approach. The effects of crystal field splitting are discussed and corresponding phase diagram are presented in Sec. III. The final section is devoted to the conclusion remarks.

II. MODEL HAMILTONIAN AND METHODS

The two-orbital Hubbard model adopted in this paper is as follows:

$$H = H_0 + H_I \quad (1)$$

$$H_0 = - \sum_{i,j\alpha\beta\sigma} (t_{\alpha\beta} c_{i\alpha\sigma}^\dagger c_{j\beta\sigma} + h.c.) + \sum_{i\alpha\sigma} (\epsilon_{i\alpha\sigma} - \mu) n_{i\alpha\sigma} \quad (2)$$

$$H_I = U \sum_{i\alpha} n_{i\alpha\uparrow} n_{i\alpha\downarrow} + \sum_{i\sigma\sigma'}^{(\alpha>\beta)} (U' - J_H \delta_{\sigma\sigma'}) n_{i\alpha\sigma} n_{i\beta\sigma'} - J_H \sum_{i\alpha\neq\beta} (c_{i\alpha\uparrow}^\dagger c_{i\alpha\downarrow} c_{i\beta\downarrow}^\dagger c_{i\beta\uparrow} - c_{i\alpha\uparrow}^\dagger c_{i\alpha\downarrow}^\dagger c_{i\beta\downarrow} c_{i\beta\uparrow}), \quad (3)$$

where $c_{i\alpha\sigma}^\dagger$ is a creation operator of an electron with the orbital index α and spin σ at the lattice site i , $n_{i\alpha\sigma}$ is the corresponding occupation number operator. The hopping integral between orbitals α and β is denoted by $t_{\alpha\beta}$. The intra-band (inter-band) Coulomb repulsion and Hund's rule coupling are denoted by U (U') and J_H , respectively. Here we set $U' = U - 2J_H$. We introduce new boson operators

*Correspondence author, Electronic mail: zou@theory.issp.ac.cn

e, p, d, b, t and q , which denote the empty, single occupation, double occupation in two orbital, double occupation in one orbital, triple occupation, and quadruple occupation, respectively. The physical electron creation operator $c_{i\alpha\sigma}^\dagger$ is represented as $Z_{i\alpha\sigma} f_{i\alpha\sigma}^\dagger$, where $f_{i\alpha\sigma}^\dagger$ is quasi-particle creation operator. The renormalization factor $Z_{i\alpha\sigma}$ is given by

$$Z_{i\alpha\sigma} = \hat{Q}_{i\alpha\sigma}^{-\frac{1}{2}} \left(p_{i\alpha\sigma}^\dagger e_i + b_{i\alpha}^\dagger p_{i\alpha\bar{\sigma}} + \sum_{\sigma'} d_{i\sigma\alpha\sigma'}^\dagger p_{i\beta\sigma'} + t_{i\alpha\sigma}^\dagger b_{i\beta} + \sum_{\sigma'} t_{i\beta\sigma'}^\dagger d_{i\bar{\sigma}\alpha\sigma'} + q_i^\dagger t_{i\alpha\bar{\sigma}} \right) (1 - \hat{Q}_{i\alpha\sigma})^{-\frac{1}{2}}, \quad (4)$$

where

$$\hat{Q}_{i\alpha\sigma} = p_{i\alpha\sigma}^\dagger p_{i\alpha\sigma} + b_{i\alpha}^\dagger b_{i\alpha} + \sum_{\sigma'} d_{i\sigma\alpha\sigma'}^\dagger d_{i\sigma\alpha\sigma'} + \sum_{\sigma'} t_{i\beta\sigma'}^\dagger t_{i\beta\sigma'} + t_{i\alpha\sigma}^\dagger t_{i\alpha\sigma} + q_i^\dagger q_i. \quad (5)$$

In the present slave boson states, the normalization constraint and Fermi number constraint maintaining physical Hilbert space are as follows:

$$1 = e_i^\dagger e_i + \sum_{\alpha\sigma} (p_{i\alpha\sigma}^\dagger p_{i\alpha\sigma} + t_{i\alpha\sigma}^\dagger t_{i\alpha\sigma}) + \sum_{\alpha} b_{i\alpha}^\dagger b_{i\alpha} + \sum_{\sigma\sigma'} d_{i\sigma\alpha\sigma'}^\dagger d_{i\sigma\alpha\sigma'} + q_i^\dagger q_i \quad (6)$$

and

$$\hat{Q}_{i\alpha\sigma} = f_{i\alpha\sigma}^\dagger f_{i\alpha\sigma}. \quad (7)$$

Our numerical method which is used to search the minima energy is based on the pattern search method, the gradient method and the Rosenbrock method. The normalization constraint given by Eq.(6) must be held at all time in our numerical calculation. The Fermion number constraint is enforced by using the penalty function method. Our numerical calculations are performed for simple square lattice with the nearest-neighbor hopping. Throughout this paper we set the ratio of two intraorbital hopping integrals as $t_{22}/t_{11} = 0.5$, and the average electron number per site is 2. We measure the energies in units of the bandwidth of the orbit-1, $2D_1 = 8t_{11}$.

III. NUMERICAL RESULTS

We first present the magnetic phase diagram of two-orbital Hubbard model at half filling as the functions of U and Δ in Fig. 1. For a large Hund's coupling, e.g. $J_H = 0.2U$, there are only paramagnetic (PM) metallic phase when $U < U_{c1}$ and AFM insulating phase for $U > U_{c1}$ in the $U - \Delta$ phase diagram. We notice that the magnetic MIT phase boundary U_{c1} shifts downward with the increase of the crystal field splitting. When the system transits from a PM metal to an AFM insulator, a fraction of electrons transfer from a lower occupied orbit to an upper unoccupied orbit. Consequently, the spin exchange splitting should overcome the crystal field splitting, leading to the decrease in the groundstate energy. We expect

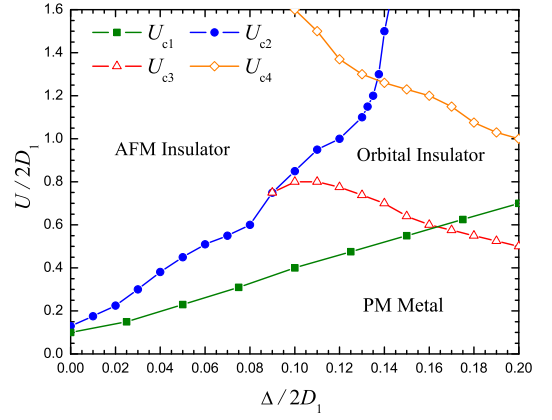


FIG. 1: Magnetic phase diagram in the $U - \Delta$ plane with $t_{12} = 0$, where U_{c1} and U_{c2} are the PM metal - AFM insulator boundary at $J_H = 0.2U$ and $J_H = 0.02U$ respectively. U_{c3} and U_{c4} are the orbital insulating phase boundaries at $J_H = 0.02U$ with and without spin degree of freedom respectively.

that the magnetic MIT is first order, since it occurs only when the spin exchange splitting is superior to the crystal field splitting. The orbital polarization induced by the crystal field splitting is also expected to decrease sharply in the AFM insulating phase.

For the small Hund's rule coupling situation with $J_H = 0.02U$, the magnetic phase diagram is richer than that with $J_H = 0.2U$. Besides the PM metallic and AFM insulating phases, an orbital insulating state is stable when $U > U_{c3}$, i.e. the system becomes completely orbital polarized without magnetism in the large Δ region. As shown in Fig.1, the present PM-AFM phase boundary U_{c2} shifts to large U , in comparison with the phase boundary U_{c1} with $J_H = 0.2U$. In the comparable large U and Δ and small J_H region, two electrons fall into the lower energy orbit. As a result, the system undergoes an AFM/PM to orbital insulator transition.

The orbital insulating phase boundary without spin correlation is also plotted as U_{c4} in Fig.1, which is in agreement with Werner and Millis' result⁴. Obviously, the present critical value for orbital insulator, U_{c3} , is considerably lower than that without spin correlation, U_{c4} , though there is no sublattice magnetic moment in the orbital insulating phase. The reason is that the modulation of spin correlation on electronic spectrum is in favor of the occurrence of the orbital insulator.

To understand the electron distributions more clearly, we present the dependence of the boson occupancy probabilities as the functions of U for different crystal field splittings in Fig.2. In the case of $J_H = 0.02U$, the spin-singlet double occupation probability b_2 is dominant over the whole correlation range when the crystal field splitting Δ is comparably large. In the case of $J_H = 0.2U$, the spin-triplet double occupation probability $d_{\sigma\sigma}$ is dominant, as seen in Fig.2. Fig.2(a) shows that when the orbital splitting $\Delta = 0$, the spin-up and spin-down occupancies split and the ground state of the system is AFM at finite U . From the inset of Fig.2(a), one notices that $d_{\uparrow\downarrow}$ considerably rises with the increase of U , since the large U and J_H are in favor of the electron distribution on

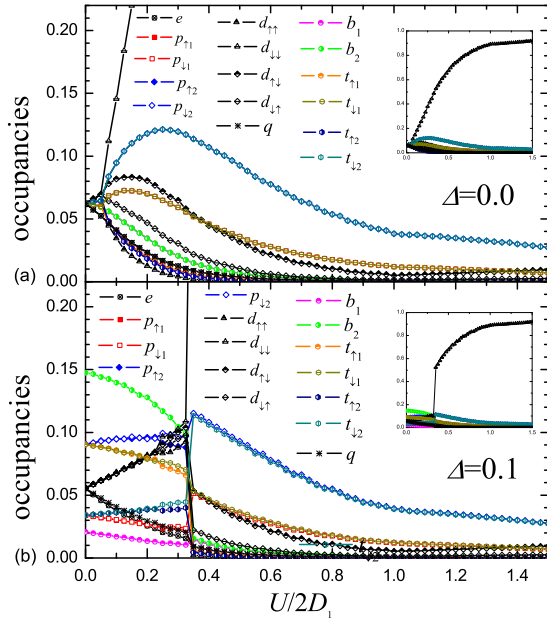


FIG. 2: Boson occupancy probabilities of sublattice as functions of U for different crystal field splitting at $n = 2$. Theoretical parameters: $J_H = 0.2U$, $t_{12} = 0.2t_{11}$. (a) $\Delta=0$; (b) $\Delta=0.1$. Insets in (a) and (b) show the full scale of the dependence of occupancies on U

different orbits with parallel spin, resulting in the dominantly increase of $d_{\downarrow\downarrow}$. And the evolution of various orbital occupancies probabilities on electron correlation qualitatively agrees with Hasegawa's results¹³.

However, in the presence of crystal field splitting, the boson occupancy probabilities shown in Fig.2(b) are very different from Fig.2(a). With increasing U , the system undergoes a first-order MIT transition and transits from PM to AFM phase at $U = U_{c1}$ since spin exchange splitting becomes larger than crystal field splitting and spin gap comes into being. At the same time, the spin-up and spin-down occupancies do not split until $U > U_{c1}$. When $U > U_{c1}$, various occupancies monotonically decrease with increasing U , except for $d_{\downarrow\downarrow}$, which steeply increases and gradually approaches a saturation, as one can see in the inset of Fig.2(b).

The evolution of the particle distributions in two orbits is plotted in Fig.3. Fig.3(a) shows that the sublattice magnetic moment contributed from narrow band is larger than that from the wide band, since the spin exchange splitting is stronger in the narrow band. In the present two-orbital system with $\Delta = 0$ and large J_H in Fig.3(a), the orbital polarization is always suppressed since the gravity centers of two bands do not shift with each other, the orbital singlet occupation dominates both in the PM metallic and in the AFM insulating phases. And from Fig.3b, it is found that although the crystal field splitting induces the partial orbital polarization in the PM metallic phase, it leads to completely unpolarized in the AFM insulating phase since the each localized electron is allocated each orbits, eliminating the orbital polarization.

The correlation dependence of the particle distributions and the renormalizations factors of two orbits at $J_H = 0.02U$ and $\Delta = 0.18$ are plotted in Fig.4(a) and (c). The corresponding

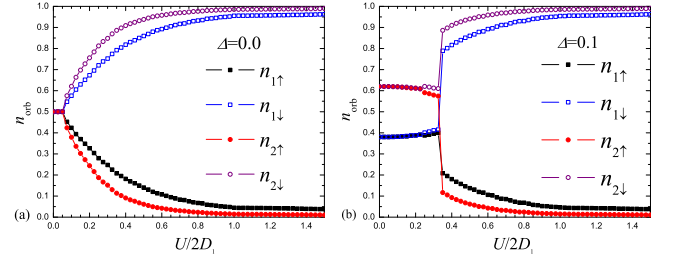


FIG. 3: Evolution of Electron number distributions in two orbits. (a) $\Delta = 0$ and (b) $\Delta = 0.1$. Other parameters are the same to Fig.2

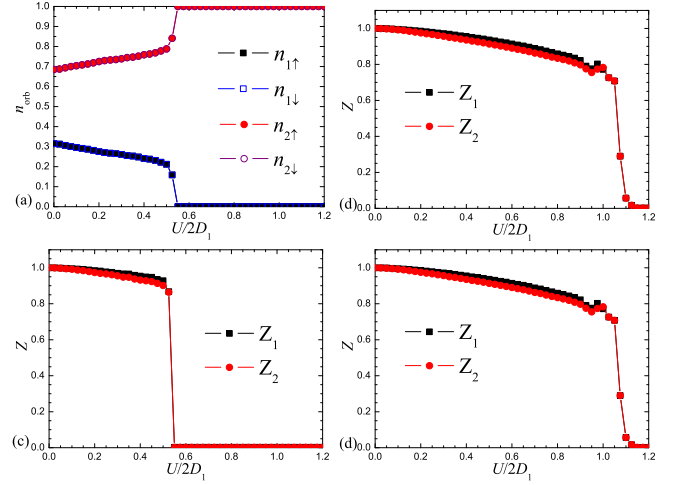


FIG. 4: Dependence of electron occupation numbers and band renormalization factors of two orbits on Coulomb correlation. (a) and (c) with spin correlation, (b) and (d) without spin correlation. Theoretical parameters: $\Delta = 0.18$, $J_H = 0.02U$, $t_{12} = 0$.

results without considering spin exchange splitting are also plotted in Fig.4(b) and (d) for comparison. Both Fig.4(a) and 4(b) show that the difference of particle numbers in two orbits, i.e. orbital polarization, increases with the increase of U , and the system becomes completely orbital polarized in the orbital insulating phase when $U > U_{c3}$, accompanied with the PM-AFM MIT. The corresponding renormalization factors in Fig.4(c) and 4(d) show that the MIT simultaneously occur in the two orbits, even if in the presence of finite crystal field splitting. Comparing Fig.4(a) with Fig.4(b) and Fig.4(c) with Fig.4(d), we find that the spin correlation greatly reduces the critical value U_c of the MIT, therefore favors the occurrence of the MIT.

Our numerical results for different inter-orbital hopping do not qualitatively affect the magnetic MIT, only the phase boundaries show a slight shift. We find that different from the statement by Yu and Si¹¹, in addition to $J_H = 0$, the orbital insulating phase can exist for finite but small J_H , since the competition between crystal field splitting and the Hund's rule coupling may stabilize the orbital insulating phase. It is interesting to expect that considerable lattice distortion may be associated with the occurrence of orbital insulator due to the first-order phase transition with large variation in orbital polarization. Further, as seen in Fig.1, 2 and 3, the high-spin to

low-spin state transition is clearly found in our present study, proving Millis *et al.*'s conjecture in their paramagnetic DMFT study⁴, which indicates that the MIT with magnetism is much more rich than that without magnetism.

IV. SUMMARY AND CONCLUSION

We have performed a comparative study on the alternative effects of crystal field splitting and Hund's rule coupling on MIT of half-filled two-orbital asymmetric Hubbard model with and without magnetism by means of the Kotliar-Ruckenstein slave boson approach. Our results show that the MIT is first order accompanied with a magnetic transition in the presence of crystal field splitting. The critical value U_c for MIT considerably reduces after taking into account the spin correlation. Meanwhile, the orbital insulator can exist in the

system with large crystal field splitting and small Hund's rule coupling. With the increase of crystal field splitting, the system may enter from a high-spin AFM state to a low-spin orbital insulating phase in the small J_H region. These results demonstrate that the competition between the crystal field splitting and the Hund's rule coupling J_H is very important for the metal-insulator transition with spin degree of freedom.

Acknowledgments

This work was supported by the National Science Foundation of China under Grant No. 10874186 and 11074257, Knowledge Innovation Program of Chinese Academy of Sciences, and Director Grants of CASHIPS. Numerical calculations were performed in Center for Computational Science of CASHIPS.

-
- ¹ A. Liebsch, Phys. Rev. Lett. 91, 22 (2003); Phys. Rev. **B 70**, 165103 (2004).
 - ² K. Bouadim, G. G. Batrouni, and R. T. Scalettar, Phys. Rev. Lett. **102**, 226402 (2009).
 - ³ A. Koga, N. Kawakami, T.M. Rice, and M. Sigrist, Phys. Rev. Lett. **92**, 21 (2004).
 - ⁴ P. Werner and A. J. Millis, Phys. Rev. Lett. **99**, 126405 (2007).
 - ⁵ E. Jakobi, N. Blümer, and P. van Dongen, Phys. Rev. **B 80**, 115109 (2009).
 - ⁶ L. de' Medici, A. Georges, and S. Biermann, Phys. Rev. **B 72**, 205124 (2005).
 - ⁷ Y. Song, L.-J. Zou, Euro. Phys. J. **B 72**, 59 (2009).

- ⁸ L. de' Medici, S. R. Hassan, M. Capone, and X. Dai, Phys. Rev. Lett. **102**, 126401 (2009).
- ⁹ A. Rüegg, M. Indergand, S. Pilgram, and M. Sigrist, Euro. Phys. J. **B 48**, 55 (2005).
- ¹⁰ X. Dai, G. Kotliar, Z. Fang, e-print arXiv: cond-mat/0611075 (2006).
- ¹¹ Rong Yu and Qimiao Si, e-print arXiv: cond-mat/1006.2337v2 (2010).
- ¹² V.I. Anisimov, I.A. Nekrasov, D.E. Kondakov, T.M. Rice, and M. Sigrist, Euro. Phys. J. **B 25**, 191 (2002).
- ¹³ H. Hasegawa, Phys. Rev. **B 56**, 1196 (1997).